Journal of Organometallic Chemistry 694 (2009) 2941–2948

Contents lists available at ScienceDirect

Journal of Organometallic Chemistry

journal homepage: www.elsevier.com/locate/jorganchem

Activation of tri(2-furyl)phosphine at a dirhenium centre: Formation of phosphido-bridged dirhenium complexes

Shishir Ghosh [a], Mansura Khatun [a], Daniel T. Haworth [b], Sergey V. Lindeman [b], Tasneem A. Siddiquee [c], Dennis W. Bennett [c], Graeme Hogarth [d,*], Ebbe Nordlander [e,*], Shariff E. Kabir [a,*]

[a] Department of Chemistry, Jahangirnagar University, Savar, Dhaka-1342, Bangladesh
[b] Department of Chemistry, Marquette University, P.O. Box 1881, Milwaukee, Wisconsin 53201-1881, USA
[c] Department of Chemistry, University of Wisconsin-Milwaukee, P.O. Box 413, Milwaukee, Wisconsin 53211-3029, USA
[d] Department of Chemistry, University College London, 20 Gordon Street, London WC1H OAJ, UK
[e] Inorganic Chemistry Research Group, Chemical Physics, Center for Chemistry and Chemical Engineering, Lund University, P.O. Box 124, SE-22100 Lund, Sweden

ARTICLE INFO

Article history:
Received 14 December 2008
Received in revised form 23 April 2009
Accepted 23 April 2009
Available online 3 May 2009

Keywords:
Rhenium
Carbonyl
Tri(2-furyl)phosphine
C–P bond cleavage
X-ray structures

ABSTRACT

Reaction of tri(2-furyl)phosphine (PFu_3) with $[Re_2(CO)_{10-n}(NCMe)_n]$ ($n = 1, 2$) at 40 °C gave the substituted complexes $[Re_2(CO)_{10-n}(PFu_3)_n]$ (**1** and **2**), the phosphines occupying axial position in all cases. Heating $[Re_2(CO)_{10}]$ and PFu_3 in refluxing xylene also gives **1** and **2** together with four phosphido-bridged complexes; $[Re_2(CO)_{8-n}(PFu_3)_n(\mu\text{-}PFu_2)(\mu\text{-}H)]$ ($n = 0, 1, 2$) (**3–5**) and $[Re_2(CO)_6(PFu_3)_2(\mu\text{-}PFu_2)(\mu\text{-}Cl)]$ (**6**) resulting from phosphorus–carbon bond cleavage. A series of separate thermolysis experiments has allowed a detailed reaction pathway to be unambiguously established. A similar reaction between $[Re_2(CO)_{10}]$ and PFu_3 in refluxing chlorobenzene furnishes four complexes which include **1**, **2**, **6** and the new binuclear complex $[Re_2(CO)_6(\eta^1\text{-}C_4H_3O)_2(\mu\text{-}PFu_2)_2]$ (**7**). All new complexes have been characterized by a combination of spectroscopic data and single crystal X-ray diffraction studies.

1. Introduction

Interest in the chemistry of tri(2-furyl)phosphine (PFu_3) stems from its potential to behave as a functionalized phosphine which has importance in transition metal catalysis [1–8]. Thus, it is well-known that heterodifunctional ligands show interesting properties such as selective binding to metal ions of different types, dynamic behavior *via* reversible dissociation of the weaker metal–ligand bond or stereoelectronic control of the coordination sphere of the metal [9]. The chemistry of phosphine ligands bearing thienyl and pyrrolyl substituents has been widely investigated due to their respective importance in the hydrodesulfurization [10] and hydrodenitrogenation [11–14] processes, and some recent developments show the striking reactivity of these phosphines towards metal carbonyl clusters [15–17]. For example, the reactivity of metal carbonyls of the iron triad with functionalized phosphines such as Ph_2PTh (Th = 2-thienyl) [17–20], Th_2PPh [21], diphenyl(benzothienyl)phosphine [21], PTh_3 [16,22,23], diphenyl(2-pyridyl)phosphine [24–35] and 2-indolylphosphine [36] has been studied by several groups, revealing that the presence of the second coordinating atom provides a diversity of coordination modes with transition metal clusters.

By way of comparison, little attention has been paid to the reactivity of polynuclear metal carbonyls and furan-containing phosphines. Wong et al. have recently reported formation of the diruthenium complex $[Ru_2(CO)_6(\mu\text{-}\eta^1,\eta^2\text{-}C_4H_3O)(\mu\text{-}PFu_2)]$, from the reaction between $[Ru_3(CO)_{12}]$ and PFu_3 at 67 °C. It results from carbon–phosphorus bond cleavage, the dissociated furyl group being coordinated to the diruthenium centre in a σ,π-vinyl fashion [37]. The reactivity of $[Ru_2(CO)_6(\mu\text{-}\eta^1,\eta^2\text{-}C_4H_3O)(\mu\text{-}PFu_2)]$ with alkynes [37] and diphosphines [38] was also documented, while we independently demonstrated its reactivity with various two-electron donor ligands, including $P(OMe)_3$, PFu_3, Bu^tNC and EPh_3 (E = P, As, Sb) [39]. Wong and co-workers have also reported a series of tetraruthenium compounds containing furyl, furyne, phosphido and phosphinidine ligands from the reaction of PFu_3 with $[Ru_4(\mu\text{-}H)_4(CO)_{12}]$ [40].

We recently reported details of the reaction between tri(2-thienyl)phosphine (PTh_3) and the dirhenium complexes $[Re_2(CO)_{10-n}(NCMe)_n]$ ($n = 0, 1, 2$) in which a series of mono- and dirhenium complexes were obtained by carbon–phosphorus and carbon–hydrogen bond activation of the ligand (**A–I**, Chart 1) [41]. As part of a study on the reactivity of functionalized phosphines with transition metal carbonyls we have now examined

* Corresponding authors. Tel.: +406 243 2592; fax: +406 243 2477 (S.E. Kabir).
E-mail address: skabir_ju@yahoo.com (S.E. Kabir).

0022-328X/$ - see front matter © 2009 Published by Elsevier B.V.
doi:10.1016/j.jorganchem.2009.04.032

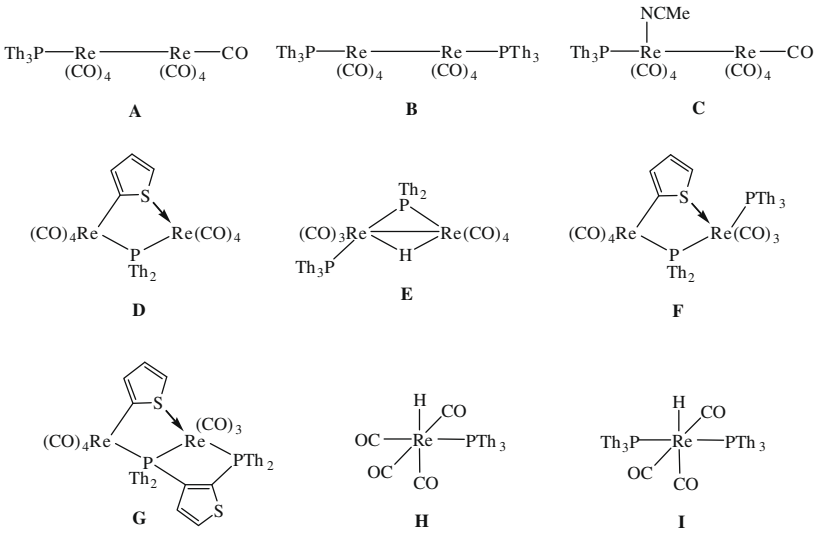

Chart 1.

the reactivity of PFu_3 towards dirhenium carbonyl compounds and observe that the reactivity of PFu_3 towards rhenium carbonyls is somewhat different from its sulfur analogue. Details of this work are described in this paper.

2. Experimental

$[Re_2(CO)_{10}]$ was purchased from Strem Chemicals Inc. and used without further purification and $[Re_2(CO)_9(NCMe)]$ and $[Re_2(CO)_8(NCMe)_2]$ were prepared according to the published procedures [42–44]. Tri(2-furyl)phosphine was purchased from Aldrich Chemical Co. and used as received. All reactions were carried out under a nitrogen atmosphere using standard Schlenk techniques. Reagent-grade solvents were dried by standard methods prior to use. Infrared spectra were recorded on a Shimadzu FTIR 8101 spectrophotometer. NMR spectra were recorded on Bruker DPX 400 and Varian Inova 500 instruments. Elemental analyses were performed by Microanalytical Laboratories, University College London.

2.1. Reaction of $[Re_2(CO)_9(NCMe)]$ with PFu_3

PFu_3 (62 mg, 0.267 mmol) was added to a benzene solution (20 mL) of $[Re_2(CO)_9(NCMe)]$ (114 mg, 0.171 mmol) and the mixture was heated to reflux for 6 h. The solvent was removed by rotary evaporation and the residue chromatographed by TLC on silica gel. Elution with hexane/CH_2Cl_2 (4:1, v/v) developed two bands which afforded the following compounds in order of elution: $[Re_2(CO)_9(PFu_3)]$ (**1**) (116 mg, 79%) as colorless crystals and $[Re_2(CO)_8(PFu_3)_2]$ (**2**) (11 mg, 6%) as yellow crystals after recrystallization from hexane/CH_2Cl_2 at 4 °C. Spectral data for **1**: Anal. Calc. for $C_{21}H_9O_{12}P_1Re_2$: C, 29.44; H, 1.06. Found: C, 29.71; H, 1.19%. IR (CH_2Cl_2): ν_{CO} = 2107 m, 2042 m, 1996 vs, 1964 m, 1943 m cm^{-1}. ^1H NMR ($CDCl_3$, 25 °C): δ = 7.73 (m, 3H), 6.73 (m, 3H), 6.53 (m, 3H). $^{31}P\{^1H\}$ NMR ($CDCl_3$, 25 °C): δ = −36.9 (s). Spectral data for **2**: Anal. Calc. for $C_{32}H_{18}O_{14}P_2Re_2$: C, 36.23; H, 1.71. Found: C, 36.49; H, 1.96%. IR (CH_2Cl_2): ν_{CO} = 2022 w, 2003 sh, 1967 vs cm^{-1}. ^1H NMR ($CDCl_3$, 25 °C): δ = 7.72 (m, 6H), 6.76 (m, 6H), 6.51 (m, 6H). $^{31}P\{^1H\}$ NMR ($CDCl_3$, 25 °C): δ = −36.6 (s).

2.2. Reaction of $[Re_2(CO)_8(NCMe)_2]$ with PFu_3

A CH_2Cl_2 solution (20 mL) of PFu_3 (70 mg, 0.301 mmol) and $[Re_2(CO)_8(NCMe)_2]$ (102 mg, 0.150 mmol) was heated to reflux for 12 h. The solvent was removed *in vacuo* and the residue chromatographed by TLC on silica gel. Elution with hexane/CH_2Cl_2 (1:1, v/v) gave **2** (116 mg, 73%).

2.3. Reaction of $[Re_2(CO)_{10}]$ with PFu_3 in xylene

A xylene solution (25 mL) of $[Re_2(CO)_{10}]$ (151 mg, 0.231 mmol) and PFu_3 (86 mg, 0.370 mmol) was heated to reflux for 12 h. The solvent was removed under reduced pressure and the residue separated by TLC on silica gel. Elution with hexane/CH_2Cl_2 (7:3, v/v) developed six bands which gave the following compounds in order of elution: $[Re_2(CO)_8(\mu\text{-}PFu_2)(\mu\text{-}H)]$ (**3**) (21 mg, 12%) as colorless crystals, **1** (18 mg, 9%), $[Re_2(CO)_7(PFu_3)(\mu\text{-}PFu_2)(\mu\text{-}H)]$ (**4**) (34 mg, 15%), **2** (49 mg, 20%), $[Re_2(CO)_6(PFu_3)_2(\mu\text{-}PFu_2)(\mu\text{-}H)]$ (**5**) (43 mg, 16%) and $[Re_2(CO)_6(PFu_3)_2(\mu\text{-}PFu_2)(\mu\text{-}Cl)]$ (**6**) (20 mg, 7%) as pale yellow crystals after recrystallization from hexane/CH_2Cl_2 at 4 °C. Spectral data for **3**: Anal. Calc. for $C_{16}H_7O_{10}P_1Re_2$: C, 25.19; H, 0.93. Found: C, 25.52; H, 1.15%. IR (CH_2Cl_2): ν_{CO} = 2108 m, 2075 m, 2009 vs, 1962 s, 1945 m, 1935 br cm^{-1}. ^1H NMR ($CDCl_3$, 25 °C): δ = 7.58 (m, 2H), 6.78 (m, 2H), 6.44 (m, 2H), −15.22 (d, J = 4.4 Hz, 1H). $^{31}P\{^1H\}$ NMR ($CDCl_3$, 25 °C): δ = −29.8 (s). Spectral data for **4**: Anal. Calc. for $C_{27}H_{16}O_{12}P_2Re_2$: C, 33.54; H, 1.67. Found: C, 33.81; H, 1.93%. IR (CH_2Cl_2): ν_{CO} = 2097 m, 2056 m, 2001 vs, 1955 s, 1931 br cm^{-1}. ^1H NMR ($CDCl_3$, 25 °C): δ = 7.74 (m, 3H), 7.60 (m, 2H), 6.89 (m, 3H), 6.79 (m, 2H), 6.54 (m, 3H), 6.42 (m, 2H), −14.46 (dd, J = 17.0, 6.0 Hz, 1H). $^{31}P\{^1H\}$ NMR ($CDCl_3$, 25 °C): δ = −41.7 (d, J_{PP} = 76.0 Hz, 1P), −21.5 (d, J_{PP} = 76.0 Hz, 1P). Spectral data for **5**: Anal. Calc. for $C_{38}H_{25}O_{14}P_3Re_2$: C, 38.97; H, 2.15. Found: C, 39.42; H, 2.32%. IR (CH_2Cl_2): ν_{CO} = 2065 w, 2044 m, 1975 vs, 1927 s cm^{-1}. ^1H NMR ($CDCl_3$, 25 °C): δ = 7.60 (m, 2H), 7.57 (m, 6H), 6.87 (m, 2H), 6.79 (m, 6H), 6.39 (m, 2H), 6.33 (m, 6H), −14.07 (dt, J = 13.2, 8.4 Hz, 1H). $^{31}P\{^1H\}$ NMR ($CDCl_3$, 25 °C): δ = −43.7 (d, J_{PP} = 78.7 Hz, 2P), −21.5 (t, J_{PP} = 78.7 Hz, 1P). Spectral data for **6**: Anal. Calc. for $C_{38}H_{24}ClO_{14}P_3Re_2$: C, 37.86; H, 2.01. Found: C, 38.22; H, 2.25%. IR (CH_2Cl_2): ν_{CO} = 2071 w, 2056 w, 1980 vs, 1914 s cm^{-1}. ^1H NMR ($CDCl_3$, 25 °C): δ = 7.63 (m, 2H), 7.59 (m, 6H), 6.90 (m, 2H), 6.85 (m, 6H), 6.41 (m, 2H), 6.36 (m, 6H). $^{31}P\{^1H\}$ NMR ($CDCl_3$, 25 °C): δ = −46.8 (d, J_{PP} = 77.2 Hz, 2P), −20.2 (t, J_{PP} = 77.2 Hz, 1P).

2.4. Reaction of $[Re_2(CO)_{10}]$ with PFu_3 in chlorobenzene

To a chlorobenzene solution (20 mL) of $[Re_2(CO)_{10}]$ (151 mg, 0.231 mmol) was added PFu_3 (86 mg, 0.370 mmol) and the mixture

was refluxed for 20 h during which time it became red. A similar chromatographic separation described as above developed five bands. The first, third and fifth bands gave **1** (16 mg, 8%), **2** (64 mg, 26%) and **6** (37 mg, 13%), respectively. The second band afforded $[Re_2(CO)_6(\eta^1\text{-}C_4H_3O)_2(\mu\text{-}PFu_2)_2]$ (**7**) (32 mg, 14%) as red crystals after recrystallization from hexane/CH_2Cl_2 at 4 °C. The content of the fourth band was too small for characterization. Spectral data for **7**: Anal. Calc. for $C_{30}H_{18}O_{12}P_2Re_2$: C, 35.85; H, 1.81. Found: C, 36.01; H, 1.96%. IR (CH_2Cl_2): ν_{CO} = 2070 s, 2026 m, 1996 vs, 1967 m cm^{-1}. ^1H NMR ($CDCl_3$, 25 °C): for both isomers: δ = 7.77 (m, 4H),

Table 1
Crystallographic data for **1**, **2** and **3**.

	1	**2**	**3**
Empirical formula	$C_{21}H_9O_{12}PRe_2$	$C_{32}H_{18}O_{14}P_2Re_2$	$C_{16}H_7O_{10}PRe_2$
Formula mass	856.65	1060.8	762.59
T (K)	100(2)	233(2)	100(2)
Crystal system	orthorhombic	orthorhombic	monoclinic
Space group	*Pbca*	*Pnna*	*P2/n*
Unit cell dimensions			
a (Å)	11.4161(2)	18.5134(6)	8.4911(2)
b (Å)	14.9954(2)	12.5098(4)	7.4590(2)
c (Å)	28.9433(4)	15.0148(5)	15.1996(3)
α (°)	90	90	90
β (°)	90	90	95.841(1)
γ (°)	90	90	90
Cell volume (Å^3)	4954.8(1)	3477.4(2)	957.67(4)
Z	8	4	2
Calculated density (g cm^{-3})	2.297	2.026	2.645
Absorption coefficient μ (mm^{-1})	19.992	14.874	25.638
F(0 0 0)	3168	2008	696
Crystal size (mm)	0.44 × 0.42 × 0.33	0.30 × 0.13 × 0.13	0.39 × 0.25 × 0.15
θ Range for data collection (°)	3.05–67.97	3.79–61.51	5.73–67.71
Index ranges	h 0/13, k 0/18, l 0/34	h 0/21, k 0/14, l 0/17	h −10/10, k 0/8, l 0/17
Completeness to θ	99.0% to 67.97°	98.9% to 61.51°	97.4% to 67.71°
Reflections collected	41 093	28 752	7807
Independent reflections	4460 (R_{int} = 0.0381)	2682 (R_{int} = 0.0252)	1690 (R_{int} = 0.0373)
Minimum and maximum transmission	0.0413 and 0.0582	0.0946 and 0.2579	0.0357 and 0.1137
Structure solution	direct methods	direct methods	direct methods
Data/restraints/parameters	4460/0/326	2682/150/218	1690/0/135
Final R indices [$F^2 > 2\sigma$]	R_1 = 0.0235, wR_2 = 0.0750	R_1 = 0.0264, wR_2 = 0.0673	R_1 = 0.0184, wR_2 = 0.0496
R indices (all data)	R_1 = 0.0236, wR_2 = 0.0751	R_1 = 0.0283, wR_2 = 0.0688	R_1 = 0.0188, wR_2 = 0.0500
Goodness-of-fit (GOF) on F^2	1.032	1.031	1.020
Largest difference peak and hole (e Å^{-3})	1.153 and −0.996	0.807 and −0.536	0.830 and −0.754

Table 2
Crystallographic data for **4**, **5**, **6** and **7**.

	4	**5**	**6**	**7**
Empirical formula	$C_{27}H_{16}O_{12}P_2Re_2$	$C_{38}H_{25}O_{14}P_3Re_2$	$C_{38}H_{24}ClO_{14}P_3Re_2$	$C_{30}H_{18}O_{12}P_2Re_2$
Formula mass	966.74	1170.9	1205.3	1004.78
T (K)	100(2)	100(2)	100(2)	100(2)
Crystal system	monoclinic	monoclinic	monoclinic	triclinic
Space group	$P2_1/c$	$P2_1/n$	$P2_1/n$	$P\bar{1}$
Unit cell dimensions				
a (Å)	8.9502(1)	10.7034(2)	9.7233(2)	9.0539(2)
b (Å)	20.0344(3)	26.0278(5)	23.0726(6)	9.5282(2)
c (Å)	16.3824(2)	14.1063(3)	17.7137(4)	10.9734(2)
α (°)	90	90	90	99.9250(10)
β (°)	94.3720(10)	97.765(1)	97.821(1)	109.3240(10)
γ (°)	90	90	90	113.4150(10)
Cell volume (Å^3)	2929.01(7)	3893.8(1)	3936.96(1)	767.63(3)
Z	4	4	4	1
Calculated density (g cm^{-3})	1.787	1.997	2.034	2.174
Absorption coefficient μ (mm^{-1})	13.256	13.738	14.221	16.742
F(0 0 0)	1488	2240	2304	474
Crystal size (mm)	0.54 × 0.25 × 0.04	0.38 × 0.13 × 0.08	0.36 × 0.19 × 0.15	0.24 × 0.19 × 0.09
θ Range for data collection (°)	3.49–67.97	3.40–67.98	3.16–67.41	4.56–67.79
Index ranges	h −10/10, k 0/23, l 0/19	h −12/12, k 0/30, l 0/16	h −11/11, k 0/26, l 0/20	h −10/9, k −11/11, l 0/13
Completeness to θ	95.9% to 67.97°	98.5% to 67.98°	98.3% to 67.41°	98.2% to 67.79°
Reflections collected	24 312	20 275	32 235	6346
Independent reflections	5107 (R_{int} = 0.0317)	6558 (R_{int} = 0.0187)	6833 (R_{int} = 0.0543)	2598 (R_{int} = 0.0163)
Minimum and maximum transmission	0.0527 and 0.6191	0.0778 and 0.4062	0.0797 and 0.2242	0.1061 and 0.3021
Structure solution	direct methods	direct methods	direct methods	direct methods
Data/restraints/parameters	5107/30/384	6558/28/509	6833/54/319	2598/0/210
Final R indices [$F^2 > 2\sigma$]	R_1 = 0.0204, wR_2 = 0.0529	R_1 = 0.0252, wR_2 = 0.0587	R_1 = 0.0641, wR_2 = 0.1791	R_1 = 0.0170, wR_2 = 0.0442
R indices (all data)	R_1 = 0.0214, wR_2 = 0.0536	R_1 = 0.0261, wR_2 = 0.0592	R_1 = 0.0763, wR_2 = 0.1865	R_1 = 0.0171, wR_2 = 0.0443
Goodness-of-fit (GOF) on F^2	1.042	1.088	1.147	1.003
Largest difference peak and hole (e Å^{-3})	0.826 and −0.769	1.159 and −0.983	2.392 and −4.289	0.770 and −0.660

7.72 (m, 2H), 7.62 (m, 7H), 7.50 (m, 3H), 6.75 (m, 1H), 6.66 (m, 6H), 6.59 (m, 1H), 6.51 (m, 1H), 6.46 (m, 9H), 6.37 (m, 5H), 6.34 (m, 1H), 6.28 (m, 3H), 6.25 (m, 1H), 6.19 (m, 1H). $^{31}P\{^1H\}$ NMR ($CDCl_3$, 25 °C): major isomer: $\delta = 92.0$ (s); minor isomer: $\delta = 91.1$ (s, 1P), 90.5 (s, 1P).

2.5. Thermolysis of *1*

A xylene solution (10 mL) of **1** (35 mg, 0.041 mmol) was heated to reflux for 3 h. Work-up and chromatographic separation as above gave three bands. The first and third bands gave **3** (12 mg, 39%) and **2** (3 mg, 7%), respectively, while the second band was unconsumed **1** (6 mg).

2.6. Thermolysis of *2*

A similar thermolysis of **2** (15 mg, 0.014 mmol) in xylene (10 mL) for 6 h. followed by similar chromatographic separation gave **4** (2 mg, 15%), **5** (6 mg, 36%) and unconsumed **2** (2 mg).

2.7. Conversion of *3* to *4*

To a xylene solution of **3** (10 mg, 0.013 mmol) was added PFu_3 (3 mg, 0.013 mmol) and the mixture was then heated to reflux for 4 h. The solvent was removed under reduced pressure and the residue chromatographed by TLC on silica gel. Elution with hexane/CH_2Cl_2 (7:3, v/v) gave **4** (4 mg, 39%).

2.8. Conversion of *4* to *5*

PFu_3 (3 mg, 0.013 mmol) was added to a xylene solution of **4** (13 mg, 0.013 mmol) the mixture was then heated to reflux for 4 h. A similar workup as above gave **5** (7 mg, 43%).

2.9. X-ray crystallographic study

Single crystals of compounds **1**–**7** suitable for X-ray diffraction were obtained by recrystallization from hexane/CH_2Cl_2 at room temperature and mounted on Nylon fibers with a mineral oil, and diffraction data were collected at 100(2) K – except for compound **2** which was studied at 233 K because of a phase transition that occurred at *ca.* 230 K – on a Bruker AXS SMART diffractometer equipped with an APEX CCD detector using graphite-monochromated Cu Kα radiation ($\lambda = 1.54178$ Å). Integration of intensities and data reduction was performed using the SAINT program [45]. Numerical (based on the real shape of the crystals) absorption correction was applied in all cases followed by the multi-scan SADABS procedure [46]. The structures were solved by direct methods [47] and refined by full-matrix least squares on F^2 [48]. All non-hydrogen atoms were refined anisotropically (Tables 1 and 2).

3. Results and discussion

3.1. Reactions of $[Re_2(CO)_9(NCMe)]$ and $[Re_2(CO)_8(NCMe)_2]$ with PFu_3

Treatment of $[Re_2(CO)_9(NCMe)]$ with PFu_3 in refluxing benzene afforded, after separation by thin layer chromatography, the substitution products $[Re_2(CO)_9(PFu_3)]$ (**1**) (79%) and $[Re_2(CO)_8(PFu_3)_2]$ (**2**) (6%) (Scheme 1). The latter could also be formed in 73% yield upon heating $[Re_2(CO)_8(NCMe)_2]$ and two equivalents of PFu_3 at 40 °C. Both were characterized by a combination of IR, ^1H NMR, elemental, and single-crystal X-ray diffraction analyses. The pattern of their IR spectra are similar to those of known mono- and di-substituted dirhenium phosphine complexes [41–44,49]. In the ^1H NMR spectra, both **1** and **2** display three equal intensity multiplets in the aromatic region, while in the $^{31}P\{^1H\}$ NMR spectra only a singlet is seen in each case. The solid-state structures are depicted in Figs. 1 and 2, respectively. In both compounds, the phos-

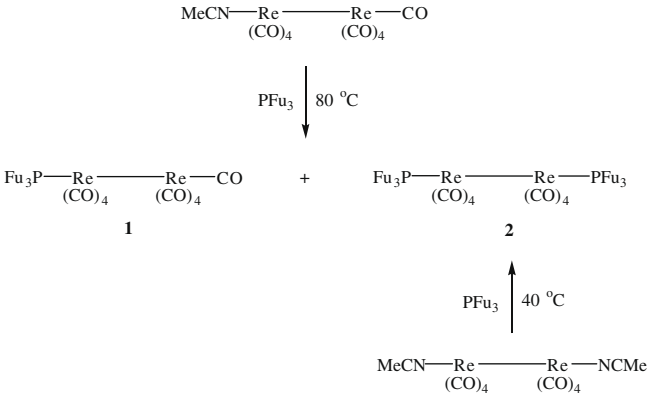

Scheme 1.

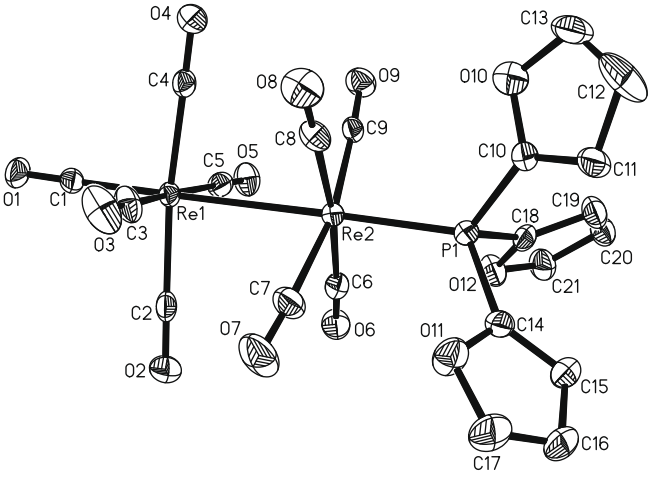

Fig. 1. Molecular structure of $[Re_2(CO)_9(PFu_3)]$ (**1**) showing 50% probability thermal ellipsoids. Ring hydrogens are omitted for clarity. Selected bond distances (Å) and angles(°): Re(1)–Re(2) 3.0281(4), Re(2)–P(1) 2.3281(14), C(1)–Re(1)–Re(2) 177.24(14), P(1)–Re(2)–Re(1) 176.62(3), C(9)–Re(2)–P(1) 93.59(13), C(8)–Re(2)–P(1) 93.47(15), C(7)–Re(2)–P(1) 97.17(16), C(6)–Re(2)–P(1) 92.65(14).

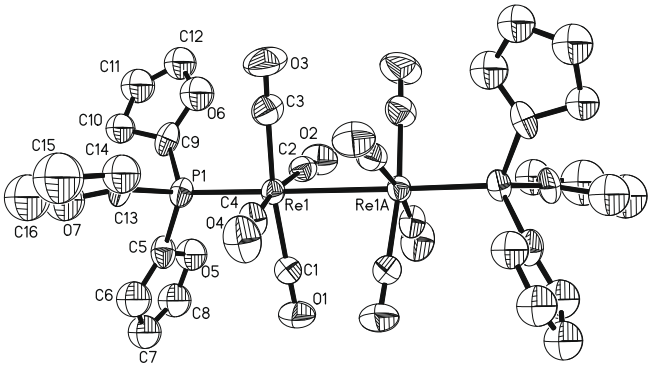

Fig. 2. Molecular structure of $[Re_2(CO)_8(PFu_3)_2]$ (**2**) showing 50% probability thermal ellipsoids. Ring hydrogens are omitted for clarity. Selected bond distances (Å) and angles(°): Re(1)–Re(1A) 3.0314(3), Re(1)–P(1) 2.3356(12), P(1)–Re(1)–Re(1A) 177.29(4), C(3)–Re(1)–P(1) 93.38(16), C(4)–Re(1)–P(1) 95.79(16), C(1)–Re(1)–P(1) 93.87(15), C(2)–Re(1)–P(1) 92.65(14), C(1)–Re(1)–C(3) 172.7(2), C(2)–Re(1)–C(4) 171.2(2).

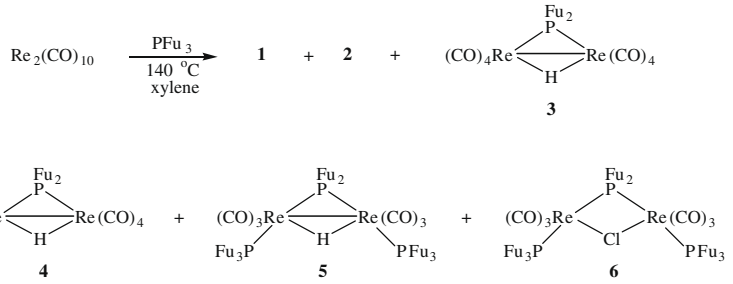

Scheme 2.

phines are axially coordinated and the rhenium–rhenium bond lengths (**1**, 3.0281(4); **2** 3.0314(3) Å) are similar to that in $[Re_2(CO)_{10}]$ (3.042(1) Å) [50].

3.2. Direct reaction of $[Re_2(CO)_{10}]$ with PFu_3: phosphido-bridged complexes via carbon–phosphorus bond cleavage

Since only phosphine coordination without further activation of the ligand was observed at moderate temperatures, we performed the direct reaction between $[Re_2(CO)_{10}]$ and PFu_3 at 140 °C in order to facilitate carbon–phosphorus bond cleavage leading to furyl coordination to the metal centres. This led to the formation of a complex mixture of products including the previously described **1** and **2** (*vide supra*) together with four new phosphido-bridged complexes, viz. $[Re_2(CO)_8(\mu\text{-}PFu_2)(\mu\text{-}H)]$ (**3**), $[Re_2(CO)_7(PFu_3)(\mu\text{-}PFu_2)(\mu\text{-}H)]$ (**4**), $[Re_2(CO)_6(PFu_3)_2(\mu\text{-}PFu_2)(\mu\text{-}H)]$ (**5**) and $[Re_2(CO)_6(PFu_3)_2(\mu\text{-}PFu_2)(\mu\text{-}Cl)]$ (**6**) (Scheme 2). Haupt et al. have previously reported the formation of $[Re_2(CO)_7(PPh_3)(\mu\text{-}PPh_2)(\mu\text{-}H)]$ and $[Re_2(CO)_6(PPh_3)_2(\mu\text{-}PPh_2)(\mu\text{-}H)]$ upon thermolysis reaction of $[Re_2(CO)_8(PPh_3)_2]$ in refluxing xylene, being isostructural with **4** and **5**, respectively [51]. Further, using toluene-d_8 as solvent they were able to show that the source of the bridging hydride is *not* the solvent, but rather originates from a PPh_3 ligand [51].

That **3**–**5** are hydride complexes is clearly seen from their ^1H NMR spectra, each of which contains a high-field signal integrating to one proton. In **3**, this appears as a doublet at $\delta = -15.22$ ($J = 4.4$ Hz), in **4** as a doublet of doublets at $\delta = -14.46$ ($J = 17.0$, 6.0 Hz) and in **5** as a doublet of triplets at $\delta = -14.07$ ($J = 13.2$, 8.4 Hz). Likewise, each compound shows a signal between δ −29.8 and −21.5 in the $^{31}P\{^1H\}$ NMR spectrum that is associated with the phosphido-bridge. Phosphine-substituted **4** and **5** also display further signals associated with the intact PFu_3 ligands, their equivalence in **5** being shown by the presence of a doublet at $\delta = -43.7$ ($J_{PP} = 78.7$ Hz). All three complexes have been characterized by X-ray crystallography, the results of which are summarised in Figs. 3–5. Each contains the same basic $Re_2(\mu\text{-}PFu_2)(\mu\text{-}H)$ core, the parameters of which are very similar. The rhenium–rhenium bond lengths [3.1447(2)–3.1604(2) Å] are significantly longer than those found in **1** and **2** or $[Re_2(CO)_{10}]$, being associated with the three-centre two-electron nature of the ReHRe interaction and better resembling values for other hydride-bridged rhenium–rhenium

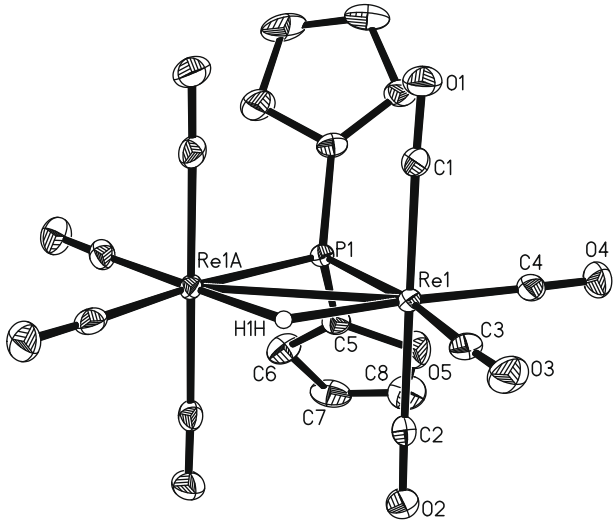

Fig. 3. Molecular structure of $[Re_2(CO)_8(\mu\text{-}PFu_2)(\mu\text{-}H)]$ (**3**) showing 50% probability thermal ellipsoids. Ring hydrogens are omitted for clarity. Selected bond distances (Å) and angles(°): Re(1)–Re(1A) 3.1571(3), Re(1)–P(1) 2.4225(10), P(1)–Re(1A) 2.4225(10), Re(1)–H(1H) 1.95(4), C(4)–Re(1)–C(3) 93.54(16), C(2)–Re(1)–C(1) 178.16(15), C(3)–Re(1)–P(1) 169.20(12), C(4)–Re(1)–Re(1A) 146.54(12), C(3)–Re(1)–Re(1A) 119.87(12), P(1)–Re(1)–Re(1A) 49.34(2), C(4)–Re(1)–H(1H) 177.1(12), C(3)–Re(1)–H(1H) 84.1(15), P(1)–Re(1)–H(1H) 85.1(15), Re(1A)–Re(1)–H(1H) 35.8(15), Re(1A)–P(1)–Re(1) 81.33(4).

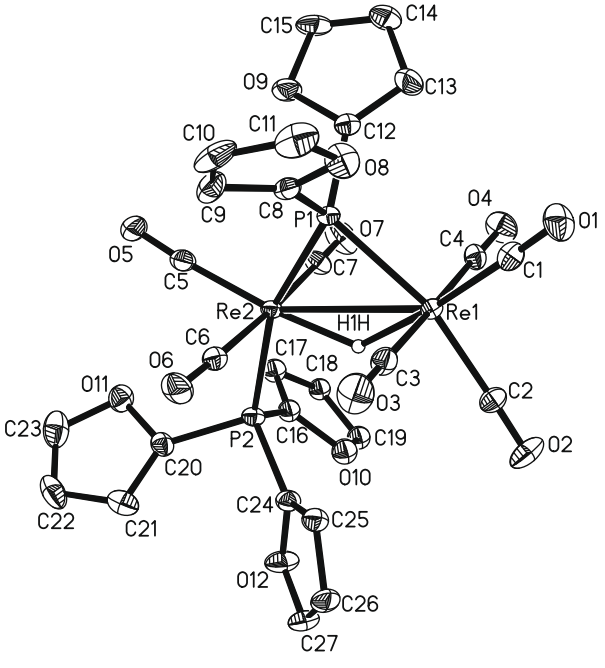

Fig. 4. Molecular structure of $[Re_2(CO)_7(PFu_3)(\mu\text{-}PFu_2)(\mu\text{-}H)]$ (**4**) showing 50% probability thermal ellipsoids. Ring hydrogens are omitted for clarity. Selected bond distances (Å) and angles(°): Re(1)–Re(2) 3.1447(2), Re(1)–P(1) 2.4212(8), Re(2)–P(1) 2.3922(8), Re(2)–P(2) 2.3802(8), Re(1)–H(1H) 1.78(6), Re(2)–H(1H) 1.72(5), C(2)–Re(1)–P(1) 163.70(10), C(2)–Re(1)–Re(2) 114.90(10), P(1)–Re(1)–Re(2) 48.808(18), P(1)–Re(1)–H(1H) 74(2), C(7)–Re(2)–C(6) 176.11(14), P(2)–Re(2)–P(1) 161.46(3), C(5)–Re(2)–Re(1) 150.82(10), C(7)–Re(2)–Re(1) 88.69(11), C(6)–Re(2)–Re(1) 95.16(11), P(2)–Re(2)–Re(1) 111.88(2), P(2)–Re(2)–H(1H) 85(2), Re(2)–P(1)–Re(1) 81.58(2).

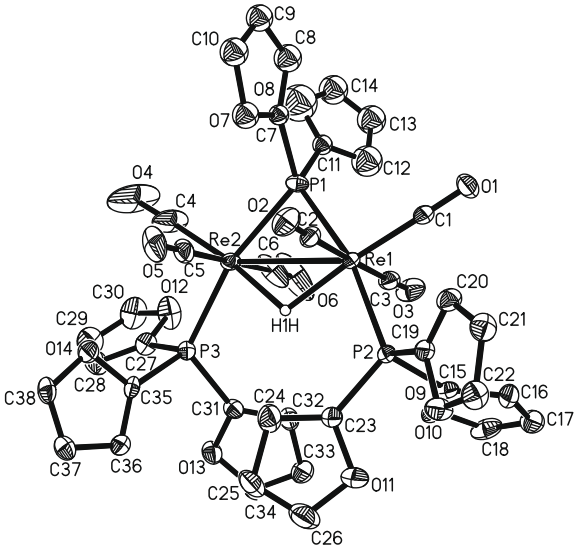

Fig. 5. Molecular structure of $[Re_2(CO)_6(PFu_3)_2(\mu\text{-}PFu_2)(\mu\text{-}H)]$ (**5**) showing 50% probability thermal ellipsoids. Ring hydrogens are omitted for clarity. Selected bond distances (Å) and angles(°): Re(1)–Re(2) 3.1604(2), Re(1)–P(1) 2.3908(10), Re(2)–P(1) 2.3972(10), Re(1)–P(2) 2.3728(10), Re(2)–P(3) 2.3723(10), Re(1)–H(1H) 1.92(5), Re(2)–H(1H) 1.98(5), C(3)–Re(1)–C(2) 178.86(17), C(6)–Re(2)–C(5) 179.3(2), P(2)–Re(1)–P(1) 166.81(3), C(1)–Re(1)–Re(2) 147.07(13), P(2)–Re(1)–Re(2) 118.24(2), P(1)–Re(1)–Re(2) 48.78(2), P(1)–Re(1)–H(1H) 85.2(16), P(3)–Re(2)–P(1) 166.24(4), C(4)–Re(2)–Re(1) 149.93(16), P(3)–Re(2)–Re(1) 119.63(3), Re(1)–P(1)–Re(2) 82.61(3).

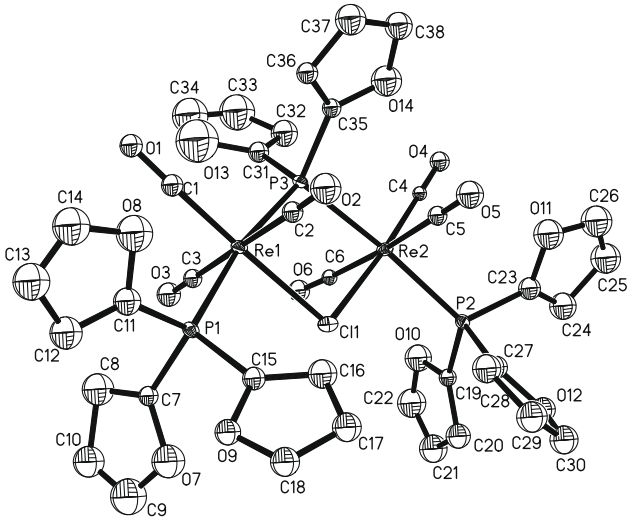

Fig. 6. Molecular structure of $[Re_2(CO)_6(PFu_3)_2(\mu\text{-}PFu_2)(\mu\text{-}Cl)]$ (**6**), showing 50% probability thermal ellipsoids. Ring hydrogens are omitted for clarity. Selected bond distances (Å) and angles(°): Re(1)–P(1) 2.393(3), Re(2)–P(2) 2.391(3), Re(1)–P(3) 2.436(3), Re(2)–P(3) 2.453(3), Re(1)–Cl(1) 2.538(3), Re(2)–Cl(1) 2.555(3), C(3)–Re(1)–C(2) 177.9(5), C(5)–Re(2)–C(6) 175.0(4), C(1)–Re(1)–P(1) 92.1(4), P(1)–Re(1)–P(3) 170.08(9), C(1)–Re(1)–Cl(1) 177.1(4), P(3)–Re(1)–Cl(1) 79.62(9), C(4)–Re(2)–P(2) 91.2(3), P(2)–Re(2)–P(3) 171.14(9), C(4)–Re(2)–Cl(1) 175.9(3), P(3)–Re(2)–Cl(1) 78.97(9), Re(1)–P(3)–Re(2) 103.52(10), Re(1)–Cl(1)–Re(2) 97.87(9).

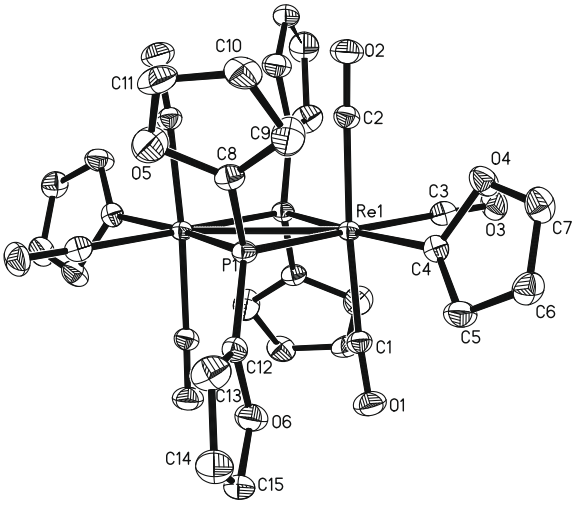

Fig. 7. Molecular structure of $[Re_2(CO)_6(\eta^1\text{-}C_4H_3O)_2(\mu\text{-}PFu_2)_2]$ (**7**) showing 50% probability thermal ellipsoids. Ring hydrogens are omitted for clarity. Selected bond distances (Å) and angles(°): Re(1)–Re(1)#1 2.9629(3), Re(1)–P(1) 2.3870(8), Re(1)#1–P(1) 2.3882(8), Re(1)–P(1)#1 2.3882(8), Re(1)–C(4) 2.153(3), C(1)–Re(1)–C(3) 88.63(14), C(1)–Re(1)–C(2) 174.54(13), C(1)–Re(1)–C(4) 86.85(13), C(3)–Re(1)–C(4) 81.80(13), C(1)–Re(1)–P(1) 92.89(10), C(4)–Re(1)–P(1) 87.57(9), C(4)–Re(1)–P(1)#1 169.09(9), P(1)–Re(1)–P(1)#1 103.30(2), P(1)–Re(1)–Re(1)#1 51.67(2), C(8)–P(1)–C(12) 101.43(16).

bonds [41]. In each, the phosphido- and hydride-bridges lie opposite one another and the substituted phosphine ligands in **4** and **5** lie *trans* to the phosphido-bridge [**4** P(2)–Re(2)–P(1) 161.46(3)°]. The molecular structure of **4** closely resembles that of $[Re_2(CO)_7(PTh_3)(\mu\text{-}PTh_2)(\mu\text{-}H)]$ (**E**) (Chart 1). In separate experiments, **1** has been shown to be the precursor to **3**, while **2** converts into **4** upon heating in boiling xylene. Likewise, **4** was also found to react with PFu_3 at 140 °C to yield **5**.

A further product of the thermolysis of $[Re_2(CO)_{10}]$ is chloride-bridged $[Re_2(CO)_6(PFu_3)_2(\mu\text{-}PFu_2)(\mu\text{-}Cl)]$ (**6**), the X-ray structure of which is depicted in Fig. 6. The molecule contains a bridging chloride ligand instead of the hydride and the metal–metal bond is absent [Re(1)–Re(2) 3.840(1) Å]. All other features of the structure are similar to that of **5**. The presence of chloride ligand in **6** is unusual but not unprecedented. We could not identify its source, but we believe that it originates from the chlorinated solvent as the yield of compound **6** is improved from 7% to 13% when the reaction was carried out in refluxing chlorobenzene which gave **1**, **2**, **6** and a new dirhenium complex $[Re_2(CO)_6(\eta^1\text{-}C_4H_3O)_2(\mu\text{-}PFu_2)_2]$ (**7**) in 8%, 26%, 13% and 14% yields, respectively (Scheme 3). No hydride complexes were obtained from this reaction. The ^1H NMR spectrum of **6** displays only aromatic resonances, while the $^{31}P\{^1H\}$ NMR spectrum closely resembles that of **5**.

The solid-state molecular structure of **7** is depicted in Fig. 7. The molecule consists of a dinuclear framework of two rhenium atoms with six carbonyls, two di(2-furyl)phosphido and two η^1-C_4H_3O ligands and possesses a centre of symmetry. The Re_2P_2 core is almost planar and the rhenium–rhenium distance of 2.9629(3) Å is

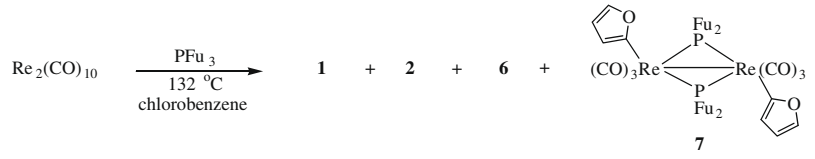

Scheme 3.

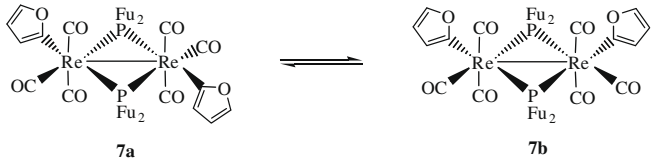

7a **7b**

Chart 2.

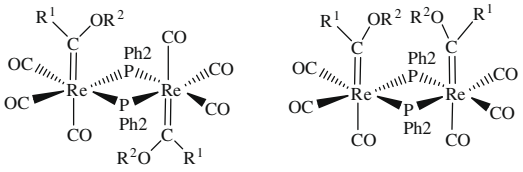

Chart 3.

considerably shorter than those observed in **3**–**5** and $[Re_2(CO)_{10}]$. The η^1-C_4H_3O ligands are equatorially coordinated to different metal centres and lie mutually *trans*. The Re–C covalent distance [Re(1)–C(4) 2.153(3) Å] is similar to those found in related complexes [18,41].

Spectroscopic data for **7** indicate that it exists in two isomeric forms in solution (Chart 2). Thus, the $^{31}P\{^1H\}$ NMR spectrum displays three resonances at $\delta = 92.0$, 91.1 and 90.5 with relative intensities of 1.5:1:1. We assume that the singlet at $\delta = 92.0$ belongs to the isomer that is found in the solid state (**7a**) whereas the singlets at $\delta = 91.1$ and 90.5 are assigned to a second isomer that we designated as **7b** (Chart 2). Complex **7** results from the oxidative addition of two carbon–phosphorus bonds to the dirhenium centre. In many ways it is a product that might be expected to form given the known propensity for cleavage of this bond, but we have not seen such a product in our previous studies [41]. Indeed we have not seen any products previously containing the $Re_2(\mu\text{-}PR_2)_2$ core. This sub-unit is fairly common, the best studied example being $[Re_2(CO)_8(\mu\text{-}PPh_2)_2]$ [52,53], although here, and in all related complexes, there is no direct rhenium–rhenium contact [53]. Most closely related to **7** are carbene complexes $[Re_2(CO)_6\{=\text{-}CR^1(OR^2)\}_2(\mu\text{-}PPh_2)_2]$ (Chart 3) which also exist as a mixture of *cis* and *trans* isomers, the rhenium–carbon bond lengths being somewhat shorter [Re–C *ca.* 2.08–2.12 Å] [54,55]. Why complex **7** should result when the thermolysis was carried out in chlorobenzene but not in xylene remains unclear. It may be that the latter provides a source of protons which results in reductive elimination of the furyl group as furan, while in chlorobenzene this pathway is prohibited. Less surprising is the increasing yield of chloro-bridged **6** (from 7% to 13%) upon using chlorobenzene and the complete absence of hydrides **4** and **5**.

From the experiments described above, a clear picture of the reaction pathway between $[Re_2(CO)_{10}]$ and PFu_3 in refluxing xylene becomes apparent (Scheme 4). It is also clear that the di(2-furyl)phosphide ligand stabilizes the dinuclear framework from degradation under forcing conditions by retaining the rhenium–rhenium bond and that it thus can be utilized in the synthesis of dirhenium complexes under vigorous reaction conditions. In all of these transformations, furyne is formally eliminated. This is not a stable entity and we have been unable to detect any organic side-products. A major difference between the chemistry described herein and the related PTh_3 chemistry [41] is the retention of the cleaved thienyl ligand upon phosphorus–carbon bond scission (see **D**, **F** and **G** in Chart 1). This may be a consequence of the stronger binding of the softer sulfur atom to the low-valent dirhenium centre.

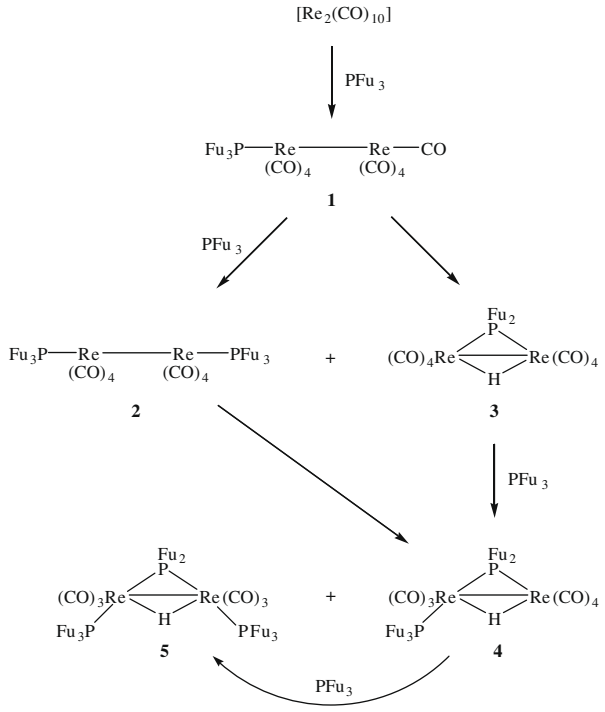

Scheme 4.

4. Supplementary material

CCDC 696083, 621643, 699655, 695316, 695317, 705767 and 726619 contain the supplementary crystallographic data for **1**, **2**, **3**, **4**, **5**, **6** and **7**. These data can be obtained free of charge from The Cambridge Crystallographic Data Centre via www.ccdc.cam.ac.uk/data_request/cif.

Acknowledgments

This research has been sponsored by the Ministry of Science and Information and Communication Technology, Government of the People's Republic of Bangladesh and the Swedish Research Council (VR).

References

[1] N.G. Anderson, B.A. Keay, Chem. Rev. 101 (2001) 997.
[2] M. Sakai, H. Hayashi, N. Miyaura, Organometallics 16 (1997) 4229.
[3] E. Shirakawa, K. Yamasaki, T. Hiyama, Synthesis (1998) 1544.
[4] B.M. Trost, Y.H. Rhee, J. Am. Chem. Soc. 121 (1999) 11680.
[5] I. Klement, M. Rottländer, C.E. Tucker, T.N. Majid, P. Knöchel, P. Venegas, G. Cahiez, Tetrahedron 52 (1996) 7201.
[6] J.C. Anderson, H. Namli, C.A. Roberts, Tetrahedron 53 (1997) 15123.
[7] W.A. Herrmann, S. Brossmer, K. Öfele, M. Beller, H. Fischer, J. Mol. Catal. A: Chem. 103 (1995) 133.
[8] V. Farina, S.R. Baker, D.A. Benigni, C. Sapino, Tetrahedron Lett. 29 (1988) 5739.
[9] K. Wajda-Hermanowicz, Z. Ciunik, A. Kochel, Inorg. Chem. 45 (2006) 3369.
[10] R.J. Angelici, in: R.B. King (Ed.), Encyclopedia of Inorganic Chemistry, vol. 3, Wiley-VCH, New York, 1994, p. 1433.
[11] R.M. Laine, Ann. N.Y. Acad. Sci. 415 (1983) 271.
[12] R.H. Fish, Ann. N.Y. Acad. Sci. 415 (1983) 292.
[13] A. Eisenstadt, C.M. Giandomenico, M.F. Frederick, R.M. Laine, Organometallics 4 (1985) 2033.
[14] M.H. Chisholm, Polyhedron 16 (1997) 3071.
[15] A.J. Arce, A.J. Deeming, Y.De. Sanctis, S.K. Johal, C.M. Martin, M. Shinhmar, D.M. Speel, A. Vassos, J. Chem. Soc., Chem. Commun. (1998) 233.
[16] U. Bodensieck, H. Varenkamp, G. Rheinwald, H. Stoeckli-Evans, J. Organomet. Chem. 85 (1995) 488.
[17] A.J. Deeming, S.N. Jaysuriya, A.J. Arce, Y. DeSanctis, Organometallics 15 (1996) 786.
[18] A.J. Deeming, M.K. Shinhmar, A.J. Arce, Y. DeSanctis, J. Chem. Soc., Dalton Trans. (1999) 1153.

[19] N.K. Kiriakidou Kazemifar, M.J. Stchedroff, M.A. Mottalib, S. Selva, M. Monari, E. Nordlander, Eur. J. Inorg. Chem. (2006) 2058.
[20] S.P. Tunik, I.G. Koshevoy, A.J. Poë, D.H. Farrar, E. Nordlander, M. Haukka, P.A. Pakkanen, J. Chem. Soc., Dalton Trans. (2003) 2457.
[21] N.K. Kiriakidou Kazemifar, M.J. Stchedroff, M.H. Johannson, M.A. Mottalib, M. Monari, E. Nordlander, unpublished results.
[22] M.A. Mottalib, S.E. Kabir, D.A. Tocher, A.J. Deeming, E. Nordlander, J. Organomet. Chem. 692 (2007) 5007.
[23] J.D. King, M. Monari, E. Nordlander, J. Organomet. Chem. 573 (1999) 272.
[24] A.J. Deeming, M.B. Smith, J. Chem. Soc., Chem. Commun. (1993) 844.
[25] A.J. Deeming, M.B. Smith, J. Chem. Soc., Dalton Trans. (1993) 3383.
[26] N. Lugan, G. Lavigne, J.-J. Bonnet, Inorg. Chem. 26 (1987) 585.
[27] V.I. Ponomarenko, T.S. Pilyugina, V.D. Khripun, E.V. Grachova, S.P. Tunik, M. Haukka, T.A. Pakkanen, J. Organomet. Chem. 691 (2006) 111.
[28] C.G. Arena, D. Drommi, F. Faraone, M. Lanfranchi, F. Nicolo, A. Tiripicchio, Organometallics 15 (1996) 3170.
[29] R. Gobetto, C.G. Arena, D. Drommi, F. Faraone, Inorg. Chim. Acta 248 (1996) 257.
[30] K. Wajda-Hermanowicz, F.P. Pruchnik, M. Zuber, G. Rusek, E. Gladecki, Inorg. Chim. Acta 232 (1995) 207.
[31] K. Wajda-Hermanowicz, M. Koralewicz, F.P. Pruchnik, Appl. Organomet. Chem. 4 (1990) 173.
[32] E. Gladecki, K. Gladecki, K. Wajda-Hermanowicz, F.P. Pruchnik, J. Chem. Crystallogr. 25 (1995) 717.
[33] K. Wajda-Hermanowicz, F. Pruchnik, M. Zuber, J. Organomet. Chem. 508 (1996) 75.
[34] F.-E. Hong, S.-C. Chen, Y.-T. Tsai, Y.-C. Chang, J. Organomet. Chem. 655 (2002) 172.
[35] D. Belletti, C. Graiff, C. Massera, G. Predieri, A. Tiripicchio, Inorg. Chim. Acta 350 (2003) 421.
[36] E. Lam, D.H. Farrar, C.S. Browning, A.J. Lough, J. Chem. Soc., Dalton Trans. (2004) 3383.
[37] W.-Y. Wong, F.-L. Ting, W.-L. Lam, J. Chem. Soc., Dalton Trans. (2001) 2981.
[38] W.-Y. Wong, F.-L. Ting, W.-L. Lam, Eur. J. Inorg. Chem. (2002) 2103.
[39] N. Begum, M.A. Rahman, M.R. Hassan, D.A. Tocher, E. Nordlander, G. Hogarth, S.E. Kabir, J. Organomet. Chem. 693 (2008) 1645.
[40] W.-Y. Wong, F.-L. Ting, Z. Lin, Organometallics 22 (2003) 5100.
[41] M.N. Uddin, M.A. Mottalib, N. Begum, S. Ghosh, A.K. Raha, D.T. Haworth, S.V. Lindeman, T.A. Siddiquee, D.W. Bennett, G. Hogarth, E. Nordlander, S.E. Kabir, Organometallics 28 (2009) 1514.
[42] U. Koelle, J. Organomet. Chem. 155 (1978) 53.
[43] G.W. Harris, J.C.A. Boeyens, N.J. Coville, J. Chem. Soc., Dalton Trans. (1985) 2277.
[44] D.R. Grad, T.L. Brown, J. Am. Chem. Soc. 104 (1982) 6340.
[45] SAINT Software for CCD Diffractometer, V.7.23A, Bruker AXS, 2005.
[46] G.M. Sheldrick, SADABS-2004/1, Program for Empirical Absorption Correction of Area-Detector Data, Institüt für Anorganische Chemie der Universität Göttingen, Germany, 2005.
[47] Program XS from shelxtl Package, V. 6.12, Bruker AXS, 2001.
[48] Program XL from SHELXTL Package, V. 6.10, Bruker AXS, 2001.
[49] W.L. Ingham, N.J. Coville, J. Organomet. Chem. 423 (1992) 51.
[50] D.W. Prest, M.J. Mays, P.R. Raithby, A.G. Orpen, J. Chem. Soc., Dalton Trans. (1982) 737.
[51] H.-J. Haupt, P. Balsaa, U. Flörke, Inorg. Chem. 27 (1988) 280.
[52] E.W. Abel, I.H. Sabherwal, J. Organomet. Chem. 10 (1967) 491.
[53] U. Flörke, M. Woyciechowski, H.-J. Haupt, Acta Crystallogr., Sect. C 44 (1988) 2101.
[54] H.-J. Haupt, D. Petters, U. Flörke, J. Organomet. Chem. 558 (1998) 81.
[55] H.-J. Haupt, D. Petters, Acta Crystallogr., Sect. E 57 (2001) m237.